J. Mar. Sci. Eng. **2015**, *3*, 1149-1177; doi:10.3390/jmse3041149

OPEN ACCESS
Journal of
Marine Science and Engineering
ISSN 2077-1312
www.mdpi.com/journal/jmse

Article

Application of a Coupled Vegetation Competition and Groundwater Simulation Model to Study Effects of Sea Level Rise and Storm Surges on Coastal Vegetation

Su Yean Teh [1,†], Michael Turtora [2,†], Donald L. DeAngelis [3,*], Jiang Jiang [4], Leonard Pearlstine [5], Thomas J. Smith III [6] and Hock Lye Koh [7]

[1] School of Mathematical Sciences, Universiti Sains Malaysia, Penang 11800, Malaysia; E-Mail: syteh@usm.my

[2] U.S. Geological Survey, Caribbean-Florida Water Science Center, 4446 Pet Lane, Suite #108, Lutz, FL 33559-630, USA; E-Mail: mturtora@usgs.gov

[3] U.S. Geological Survey, Southeast Ecological Science Center, Coral Gables, FL 33124, USA

[4] Jiang Jiang, Forestry College of Nanjing Forestry University, Key Laboratory of soil and water conservation and Ecological Restoration, Nanjing Forestry University, Nanjing 210037, China; E-Mail: ecologyjiang@gmail.com

[5] Leonard Pearlstine, Everglades National Park, South Florida Natural Resources Center, 950 N Krome Ave, Homestead, FL 33030, USA; E-Mail: Leonard_Pearlstine@nps.gov

[6] U.S. Geological Survey, 600 Fourth Street South, St. Petersburg, FL 33701, USA; E-Mail: tom_j_smith@usgs.gov

[7] Hock Lye Koh, Sunway University Business School, Jalan Universiti, Bandar Sunway, Selangor 47500, Malaysia; E-Mail: hocklyek@sunway.edu.my

† These authors contributed equally to this work.

* Author to whom correspondence should be addressed; E-Mail: don_deangelis@usgs.gov; Tel.: +1-305-284-1690.

Academic Editor: Rick Luettich

Received: 31 July 2015 / Accepted: 21 September 2015 / Published: 25 September 2015

Abstract: Global climate change poses challenges to areas such as low-lying coastal zones, where sea level rise (SLR) and storm-surge overwash events can have long-term effects on vegetation and on soil and groundwater salinities, posing risks of habitat loss critical to

native species. An early warning system is urgently needed to predict and prepare for the consequences of these climate-related impacts on both the short-term dynamics of salinity in the soil and groundwater and the long-term effects on vegetation. For this purpose, the U.S. Geological Survey's spatially explicit model of vegetation community dynamics along coastal salinity gradients (MANHAM) is integrated into the USGS groundwater model (SUTRA) to create a coupled hydrology–salinity–vegetation model, MANTRA. In MANTRA, the uptake of water by plants is modeled as a fluid mass sink term. Groundwater salinity, water saturation and vegetation biomass determine the water available for plant transpiration. Formulations and assumptions used in the coupled model are presented. MANTRA is calibrated with salinity data and vegetation pattern for a coastal area of Florida Everglades vulnerable to storm surges. A possible regime shift at that site is investigated by simulating the vegetation responses to climate variability and disturbances, including SLR and storm surges based on empirical information.

Keywords: coupled hydrology–vegetation model; salinity; coastal Everglades; hardwood hammock; mangroves; vadose zone; groundwater

1. Introduction

Sea Level Rise (SLR) is one of the most significant predicted consequences of global climate change and has the potential for severe effects on the vegetation of low-lying coastal areas and islands [1]. Rising sea level will also mean higher storm surges [2], even if the frequencies do not change. Mean SLR will have a gradual effect on shoreline retreat and subsequent loss of ecosystem area in these locations. However, large-scale marine water intrusion through storm surges may affect large areas on a short time scale, including the inundation of whole low-lying islands. The immediate effect will be on the freshwater lenses that sit on top of saline groundwater in these areas. Such effects on available fresh water may have negative consequences for the ecological and human populations of coastal areas and, particularly, islands, as they depend critically on fresh water stored in the lenses [3–5]. Longer-term consequences may involve large-scale vegetation regime changes, which can pose risks to conservation and restoration efforts in coastal national parks and preserves. For example, in southern Florida, USA, the beneficial effects of increased freshwater flow resulting from the Comprehensive Everglades Restoration Plan (CERP) [6] may be compromised in some places by increased saltwater intrusion and salinity overwash events.

In tropical and subtropical coastal areas, increase in salinity of the vadose zone (unsaturated soil zone) induced by storm surges might reduce or eradicate the salinity-intolerant (glycophytic) species and promote rapid landward migration of salinity-tolerant (halophytic) species such as mangroves. Inland expansion of mangroves at the expense of glycophytic vegetation has been noted in coastal ecosystems, e.g., see [7,8]. The effect of a disturbance may cause a rapid shift in the transition zone between vegetation types, also called the ecotone [9]. While many ecotones between floristic types are broad and diffuse, some are remarkably narrow. An example of the sharpening of ecotones in coastal areas involves halophytic vegetation (mangrove vegetation in tropical and sub-tropical regions) and glycophytic

vegetation (including tropical hardwood trees forming "hammocks", and freshwater marsh) in southern Florida coastal areas [10]. Typically, these are not interspersed. Stability of the ecotone is promoted by self-reinforcing positive feedback as follows [11]. During the dry season, plant transpiration can lead to infiltration by highly brackish underlying ground water into the vadose zone. Hardwood hammock trees reduce transpiration when the salinity in the vadose zone increases. This limits the salinization of the vadose zone. Meanwhile, the transpiration of mangroves can continue even at relatively high salinities, sustaining salt-water infiltration. Thus, through self-reinforcing positive feedback, each type of vegetation has a tendency to promote the salinity condition that is favorable to itself in competition.

However, both SLR over decades and the acute effects of large storm surges may upset that stability. If a large enough pulse of salinity from overwash remains in the soil for a long period, it may overwhelm the feedback maintaining the favorable conditions for glycophytic vegetation, such that the ecotone can no longer be maintained; that is, a regime shift could occur. Large areas of glycophytic vegetation could be replaced by halophytic vegetation, which may lead to permanent salinization of the vadose zone. For example, Baldwin and Mendelssohn [12] studied the effects of salinity and inundation coupled with clipping of aboveground vegetation on two adjoining plant communities, *Spartina patens* and *Sagittaria lancifolia*. The study reported that that the levels of flooding and salinity at the time of disturbance determined the potential shift of vegetation to a salt tolerant species. Large storm surges created by Hurricanes Katrina and Rita (2005) affected the coastal areas of Louisiana, USA. Subsequently, both freshwater and brackish communities exhibited changes in vegetation [13]. It was noted that in the central region of their study area, marsh composition changed to a more saline classification, and high mean salinities exceeded mean pore-water salinity levels tolerated by the previous dominant species.

Hindcasting the effects of previous storm surges and on coastal vegetation and forecasting the future effects of both storm surges and SLR requires modeling. In particular, forecasting these effects on the halophyte-glycophyte ecotone requires that the competition of these two vegetation types be modeled along with hydrology and salinity dynamics. To investigate the dynamics of the ecotone between halophytic and glycophytic vegetation, including the possibility of a regime shift, a spatially explicit computer simulation model, MANHAM (MANgrove HAMmock model), has been developed [14].

MANHAM simulates the competition of hardwood hammock trees and mangrove trees on a grid of spatial cells; each a few square meters in area. Vegetation of each type may be present in a given cell, and growth and competition are modeled on this local scale. Dispersal of propagules of each species is also modeled. In cells where vadose zone salinity is low, hammock trees grow faster and outcompete mangroves, but in higher salinity cells, hammock tree growth is slowed and mangroves can outcompete the hammock trees.

MANHAM also models water flow and salinity in the vadose zone, which depends on precipitation, tides, evaporation, plant transpiration, and groundwater infiltration. The dynamics of hydrology and salinity are modeled on a time resolution of less than a day, whereas the dynamics of vegetation is modeled on monthly time steps. The key mechanism in the model is the self-reinforcing positive feedback relationship between each vegetation type and vadose zone salinity described above. In each spatial cell these feedbacks help maintain dominance of the current vegetation type in the cell, hammock or mangrove, against invasion by the other type. However, a large external impact on the vadose zone salinity of a cell dominated by hammock trees, such as from storm surge overwash, could lead to decline in hardwood growth and favor growth of mangrove propagules, or seedlings, into trees. Through positive

feedback between the growing mangrove vegetation and the vadose zone salinity, the cell could eventually shift to mangrove domination. Shifts from mangrove to hardwood hammock are also possible if there is a sufficient external forcing of freshwater. Mathematical details of MANHAM are described in Appendix 1.

MANHAM has examined the impact of SLR on southern Florida coastal forests [15], showing that buttonwood forest (*Conocarpus erectus*), could be squeezed out by red mangrove (*Rhizophora mangle*). Simulations have also indicated that a significant one-day storm surge event could feasibly initiate a vegetation shift from hardwood trees to mangroves in areas initially dominated by the former. Mangroves in the model were able to take over large areas when storm surges saturated the vadose zone with over 0.015 kg/kg salinity, if the salinity was not quickly washed out of the vadose zone by precipitation, and if a sufficient density of mangrove propagules (seedlings, by which mangroves are spread) were present. It was observed that such a shift might not be conspicuous at first, but would be inevitable once a tipping point had been passed. These findings are relevant to many coastal areas, including the coastal Everglades. They have motivated us to apply the modeling to forecasting future changes in coastal vegetation and developing plans to meet the challenges of these changes.

MANHAM simulates the vadose zone as a uniform compartment and does not model underlying groundwater dynamics [14] and assumes that ground water is a constant boundary condition. These assumptions are certainly violated in real systems. For example, in low-lying coastal areas and small atoll islands, tides cause diurnal fluctuations in groundwater, and storm surges can cause major changes in groundwater that can last for years. A deficiency caused by these assumptions in MANHAM is that it does not consider the freshwater lens, which in coastal areas and atolls typically overlies deeper water salinity levels of the neighboring seawater. This freshwater lens is an important constituent of the water balance for the overlying vegetation through transpiration and plays a key role on the salinity balance as well. Because of these deficiencies we developed MANTRA (MANhamsuTRA), which builds in more detailed hydrological and salinity dynamics. Below we describe the USGS's Saturated–Unsaturated TRAnsport (SUTRA) groundwater model and its coupling with MANHAM to form MANTRA. We apply MANTRA to a coastal area of Everglades National Park (ENP), southern Florida, and demonstrate how it can be used to project the effects of both storm surges and SLR on coastal vegetation.

2. Methods

2.1. MANTRA Model

To overcome the limitation due to MANHAM's lack of a freshwater lens, MANHAM has been integrated with an established groundwater hydrology and salinity model, the United States Geological Survey (USGS)'s Saturated–Unsaturated TRAnsport (SUTRA) groundwater model [16,17]. The fluid pressure and salinity gradients in the transition zone between glycophytic and halophytic vegetation associated with the freshwater lens are quantified by the variable density flow simulated by SUTRA. SUTRA also simulates the unsaturated zone of the soil, and so can substitute for the hydrodynamics and salinity dynamics of the soil and groundwater. However, SUTRA does not include vegetation competition dynamics. By combining MANHAM with SUTRA, forming MANTRA (MANhamsuTRA), we provide an integrated model that simulates the possible effects of gradual SLR, as well as both

short- and long-term effects of a single or a sequence of overwash events on a coastal area or small island, containing zones of glycophytic and halophytic vegetation.

MANTRA input data are (1) vegetation type and (2) groundwater conditions (fluid pressure and salinity) and it simulates the changes in vegetation type biomass over time subject to the groundwater conditions. Because MANTRA is an extension of SUTRA, it also delivers the output of SUTRA, including fluid pressure and solute concentration. The primary variable upon which the groundwater model SUTRA is based is fluid pressure, which varies spatially and temporally. Variations in fluid density and fluid pressure differences drive flow of groundwater, which is a fundamental mechanism upon which the solute transport model is based. MANTRA employs spatial discretization called mesh by quadrilateral finite elements. In a cross sectional form, the elements are organized in rows and columns with each element having four nodal points. Nodal points (or nodes) are shared by the elements adjoining the node. A cell is centered on a node, not an element. Cell boundaries are half way between opposite sides of an element as shown in Figure 1. Further details of MANTRA are described in Appendix 2.

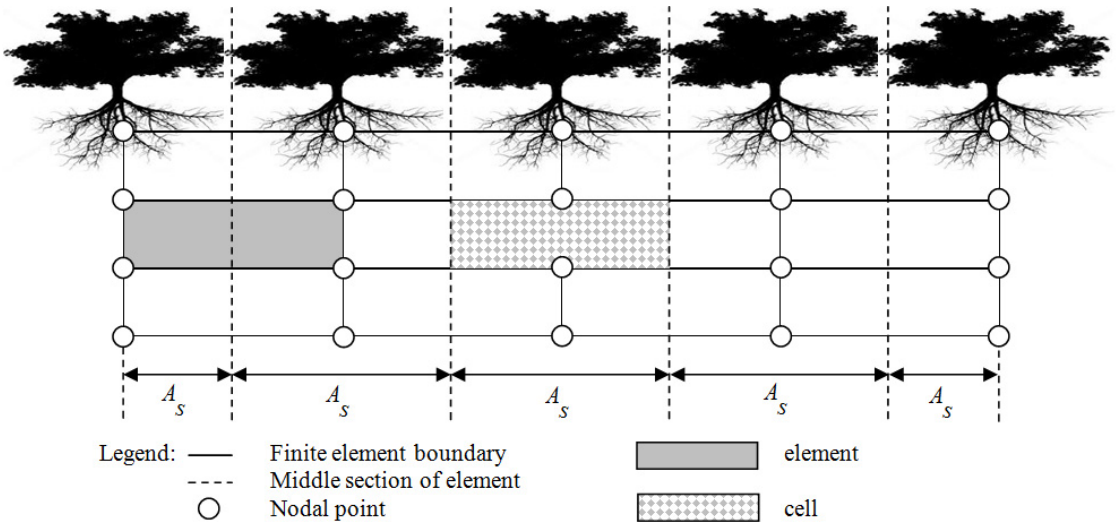

Figure 1. Schematic sketch of a hypothetical simulation case for illustration purposes.

Here we describe an important aspect of how the hydrology of SUTRA and the vegetation dynamics of MANHAM interact, which is through water uptake by plants. The fluid mass source/sink term Q [M/s] (where M = mass and s = second) in SUTRA, which accounts for external addition/subtraction of fluid including pure water mass plus the mass of any solute dissolved in the source fluid, can be used to characterize the uptake of water by plants (Q_p) [18–20]. This term in a mass balance equation is used to represent the addition (source) or extraction (sink) from the mass balance system. As a function of salinity, the total water uptake $R = f(C)$ [L/s] (where L here is the dimension of vertical distance or depth) by plants is determined by the salinity concentration C [M_s/M_f] (where M_s = mass of solute and M_f = mass of fluid) calculated by SUTRA. The salinity C is derived from the solute mass balance equation that includes processes such as fluid flow and diffusion. Then, assuming a closed canopy so that transpiration can be assumed constant for the vegetation types and evaporation ignored, the fluid mass per unit time (Q_p) required by the plants in a certain horizontal cell for transpiration can be estimated by:

$$Q_p = R \cdot A_s \cdot \rho \text{ [M/s]} \quad (1)$$

Here, A_s represents the surface along the depth dimension [L^2] and ρ is the fluid density of fresh water [M/L^3]. For cross-sectional model, the width of each cell is assumed to be 1.0 m. Thus, A_s depends on the length or horizontal grid size (Figure 1).

It may happen that the fluid mass required by the plant for transpiration is more than what is available (unsaturated flow). Hence, there should be a relation between the fluid mass required by transpiration and the fluid mass available. It is assumed that actual fluid mass being subtracted from a cell due to transpiration depends on the saturation S_w and porosity ε in the cell, leading to the following relation:

$$Q_{IN} = -Q_p \cdot \varepsilon \cdot S_w \text{ [M/s]} \quad (2)$$

where, Q_{IN} = total mass sink (due to plant transpiration) [M/s]; ε = porosity [V_v/V]; S_w = water saturation [V_w/V_v] with V = total volume, V_v = volume of voids, V_w = volume of water. Suppose porosity ε is kept constant at 1.0. When the void space is completely filled with fluid and is said to be saturated, that is $S_w = 1$, the actual water uptake by plants, Q_{IN}, will be equivalent to the amount of water required by the plants, Q_p. When the void space is only partly water filled and is referred to as being unsaturated, that is $S_w < 1$, the actual water uptake by plant will decrease as a factor of the saturation, S_w.

To simulate fluid inflow to the soil pores due to seawater inundation during a storm surge, Equation (3) below [21] was used to specify the pressure at surface nodes inundated by seawater.

$$p = \rho_{sea} \cdot g \cdot h \quad (3)$$

Here, p = pressure at top layer nodes [$M/(Ls^2)$], ρ_{sea} = fluid density of seawater [M/L^3], g = gravity [L/s^2], h = inundation depth [L].

2.2. Study Transect

To evaluate MANTRA's effectiveness in a coastal Everglades setting, we chose a site and a set of scenarios related to past and possible future events. MANTRA was used on a coastal site that has been exposed to storm surges. The main objective of MANTRA is to project possible future changes in hardwood hammocks in southern Florida under conditions of gradually rising sea level and/or major storm surges. As an example, we apply MANTRA to a specific hardwood hammock along the southwestern coast of ENP, bordering Florida Bay (25°12′24.13″ N, 80°55′47.48″ W). This hammock has been described by Saha *et al.* [22], where it is referred to as the Coot Bay Hammock (see aerial view in Figure 2). The hammock is in the middle of a low ridge with north-south orientation. Along a 370 m transect from west to east across the hammock (see Figures 2 and 3), vegetation changes from black mangroves (*Avicennia germinans*) at the low elevation (0.4–0.5 m above mean sea level) western end to mixed halophyte coastal prairie (*Batis/Salicornia*) (0.5–0.7 m) with individual buttonwoods (*Conocarpus erectus*) (0.7–0.8 m), to mixed-hammock, and hardwood hammock communities (0.9–1.5 m) at the peak in elevation in the middle of the ridge. As one continues farther along the transect, the associations occur in reverse order, except for a change from white to black mangroves. The transitions are relatively sharp. The geology is marl mixed with peat to a depth of 2–3 m over karst bedrock. Table 1 shows assumed ranges of conductivities. The site has a tropical climate with an average of 1570 mm annual precipitation, nearly 60% of which is from June through September. Mean January and

July temperatures are, respectively, 22 °C and 30 °C. Hourly salinity data of water at 0.5 m below land surface were available at two locations (blue dots near transect on Figure 2) and monthly point measurements of salinity and water depth at five locations (other blue dots on Figure 2) from in February 2011, through July 2012. Coot Bay Hammock is an ideal study transect because hardwood hammocks occur at the highest, and mangroves and coastal prairies occur at the lowest end of the gradient in elevation.

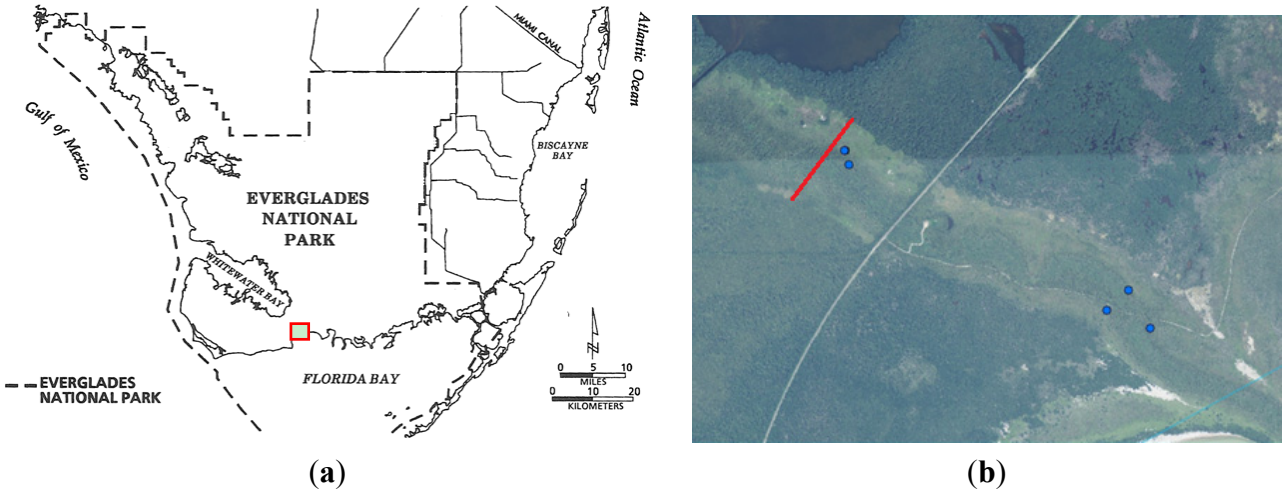

Figure 2. (**a**, **Left**) Southern Florida with site shown in red box (from Light and Dineen 1994 [23]). (**b**, **Right**) Aerial view of Coot Bay Hammock, with 370 m transect, shown in red. Blue dots indicate well sites. l. (Figure 2a adapted from reference [23] with copyright permission).

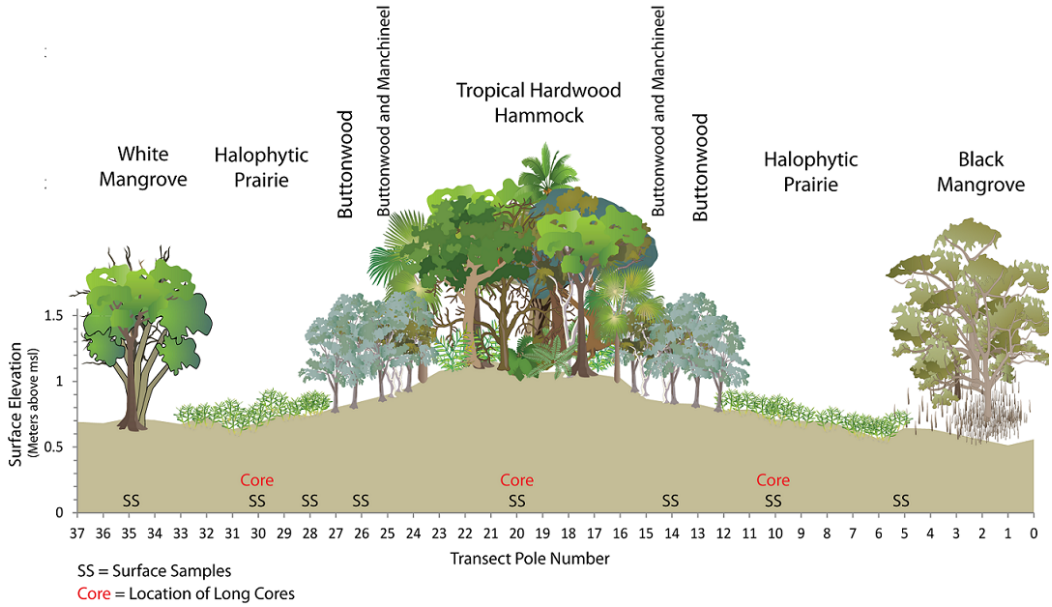

Figure 3. West-to-east transect of about 370 m across the Coot Bay Hammock showing the sharp gradations between vegetation types. Transect poles mark 10 m distances, and locations where surface samples and core samples were taken. Figure courtesy of Brandon Gamble, National Park Service. Graphic symbols courtesy of the Integration and Application Network, University of Maryland Center for Environmental Science.

Table 1. Stratigraphy and hydraulic conductivities used for the Coot Bay Hammock. Parameter values are assumed from other sources.

Layer Name	Lower Boundary (m)	Hydraulic Conductivity (Qualitative) (m/Day)	
Marl plus peat	~2–3	low	<0.3
karst	~6	high	>1000
sand	~9	medium	10 to 100
noflow	~9		

Saha *et al.* [22] noted an increase in salinity over the last decade (data from hydrological station maintained by ENP). Saha *et al.* [22] suggest that SLR can induce a rising water table, which will cause a shrinking of the vadose zone and an increase in salinity in the bottom portion of the freshwater lens, subsequently increasing brackishness of plant-available water. For these reasons, the Coot Bay Hammock was selected as a first site to test MANTRA. The 370 m transect was modeled as two-dimensional, with the horizontal dimension along the transect, and the vertical axis for depth.

Storm surge/SLR would most likely occur from the lower right of Figure 2, right panel. This happened in November 2005 due to Hurricane Wilma [24]. A storm surge could also enter the area through a canal system. The park road through ENP to the town of Flamingo on Florida Bay (visible in Figure 2) cuts across the southern tip of the tropical hardwood forest that extends to the NW. The ridge extends further SE with vegetation that was identified in 1981 as "collapsed hammock" [22] and is now referred to as a transitional buttonwood hardwood hammock.

The Coot Bay Hammock area is vulnerable to both wind damage and storm surges from hurricanes. Hurricanes have been important in shaping the vegetation of the region. The "Labor Day" hurricane of 1935 killed many buttonwoods, while Hurricane Donna (1960) produced a storm surge of 4 m in this area, causing 90% mortality of trees on lower ground, and 25%–50% mortality buttonwoods and hardwood hammock trees on coastal hammocks such as the Coot Bay Hammock. These hurricanes were factors that "produced new vegetation mosaics of white, black and red mangroves and buttonwoods" [25]. Buttonwoods have not recovered in some areas they once dominated. While fires have been suggested as a possible factor in their loss, Olmstead and Loope [25] discount this, which leaves open the possibility that a storm surge induced regime shift was the cause. Two hurricanes that more recently have affected the Coot Bay Hammock area were Hurricane Andrew (1992) and Hurricane Wilma (2005). The storm surge from Andrew measured 1.2–1.5 m at Flamingo, near Coot Bay Hammock, while that from Wilma measured 0.7 m at Black Forest, also near Coot Bay Hammock, see [26]. Hurricane Andrew caused very little structural damage to trees that far south, while Wilma caused moderate though not severe damage.

2.3. Model Simulations

A 2-D model of the transect across the Coot Bay Hammock was developed using MANTRA. For simplicity, buttonwoods were aggregated with the hardwood hammock, and hardwood hammock and mangroves were modeled as competing vegetation types. Coastal hammocks, tree islands, and buttonwood forests of Florida Bay experience tidal amplitude of only ~15 cm [27], so tides were ignored in the model. Model scenarios are described below.

2.3.1. Scenario 1: Existing Conditions

The model was first applied to the existing conditions of the Coot Bay Hammock. The aim was to calibrate the model to produce results that are consistent with the observed data; that is, with the observed sharp boundary and with virtually no mangroves in areas dominated by hardwood hammocks and *vice versa*.

2.3.2. Scenarios 2 and 3: Storm Surges

Preliminary MANTRA simulations (not shown here) showed that neither of the storm surges plus the associated light damage to the hammock from Hurricanes Andrew and Wilma would be sufficient to cause a regime shift from hardwood hammock to mangroves. However, sites such as Coot Bay Hammock have been struck by larger hurricane disturbances in the more distant past, and will be in the future. Therefore, to project the effects of greater disturbances, two storm surge scenarios were applied that used inundation depths consistent with those caused by Hurricane Andrew, *i.e.*, about 1 m, but which had some additional factors that would amplify the effects of the surge. Scenario 2 assumes that the storm inflicted heavy damage to the hardwood hammock trees, reducing their living biomass to below the level of mangrove seedlings. Scenario 3 consisted of a storm surge in which only moderate damage was done to the hardwood hammock vegetation, reducing the initial vegetation by one-half. However, the storm surge was followed immediately by a severe four-year drought in which mean precipitation was reduced by half. Although a four-year drought starting immediately following a hurricane would be unusual, periodic droughts are part of the climate of southern Florida, and a drought of this magnitude is plausible.

2.3.3. Scenario 4: Gradual SLR

A final scenario (Scenario 4) of gradual SLR was applied over a period of 150 years without storm surge events.

3. Results

3.1. Scenario 1: Existing Conditions

The results for the distribution of mangroves and hardwood hammock trees for the calibrated MANTRA are shown in Figure 4. Consistent with the vegetation distribution observed at the Coot Bay Hammock, our results show the hardwood hammocks occupy the slightly elevated ridge, where a freshwater lens of about 0.5 m is maintained by precipitation and feedback from hardwood hammocks, whereas the mangroves occupy the lower elevated areas on either side of the hardwood hammock area.

3.2. Scenarios 2 and 3: Storm Surges

Next, storm surge Scenario 2 was applied using MANTRA. The results of the simulation are shown in Figure 5. The process of the positive feedback involving increased mangrove invasion causing increased soil salinity, allowed the mangroves to take over in about 16 years. Scenario 3 consisted of a storm surge in which only moderate damage was done to the hardwood hammock vegetation, but was

followed by a severe four-year drought. The results are shown in Figure 6, where again the mangroves took over the entire site within about 16 years. Again, the positive feedback loop of mangrove invasion and increasing salinity drove the transition.

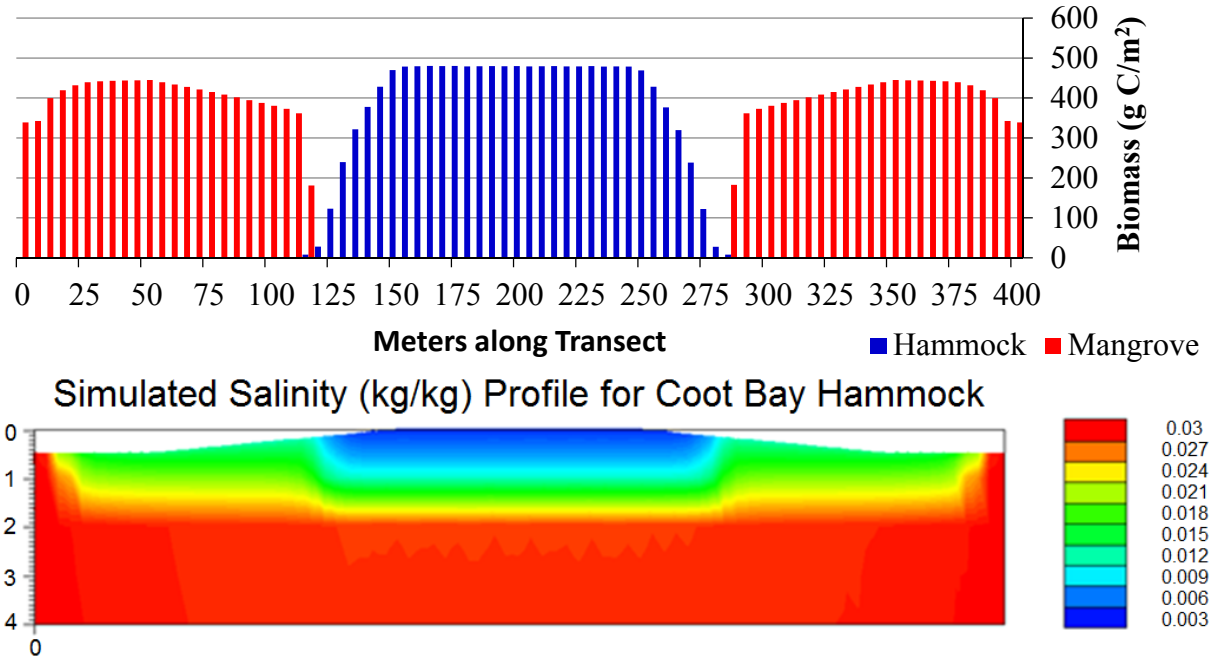

Figure 4. (**Top**) Simulated distribution of mangroves (red) and hardwood hammock (blue) trees along a 370-meter transect (rounded to 400 m in the model) across the Coot Bay Hammock. (**Bottom**) Simulated salinity profile with ground depth in meters and salinity in kg/kg.

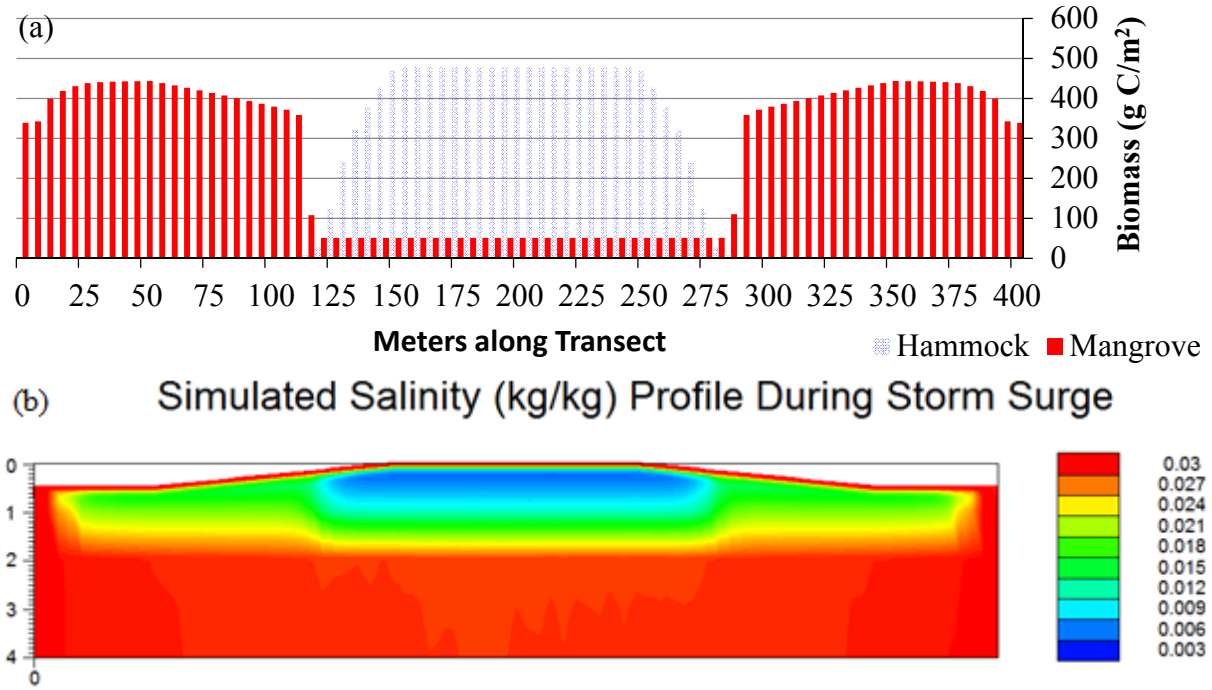

Figure 5. *Cont.*

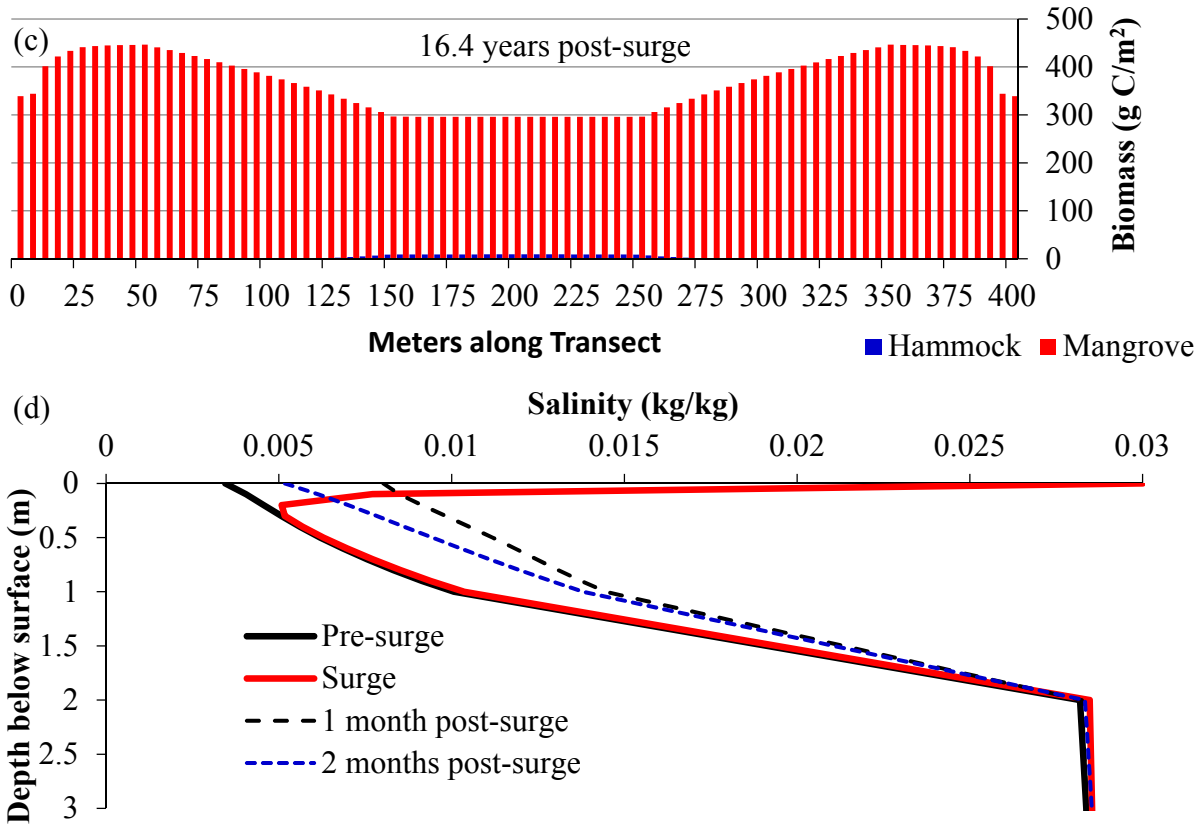

Figure 5. (**a**, **Top**) Depiction of initial conditions following storm surge, with almost complete elimination of hardwood hammock living biomass through knockdown of trees. Faded blue colors indicate destruction of initial trees. (**b**, **Second from top**) Simulated salinity profile during the storm surge. (**c**, **Third from top**) Simulated distribution of mangrove (red) vegetation 16.4 years (6000 days) after the storm surge. (**d**, **Bottom**) Sequence of salinity profiles starting before the surge until two months after, as predicted by MANTRA, with the particular precipitation pattern.

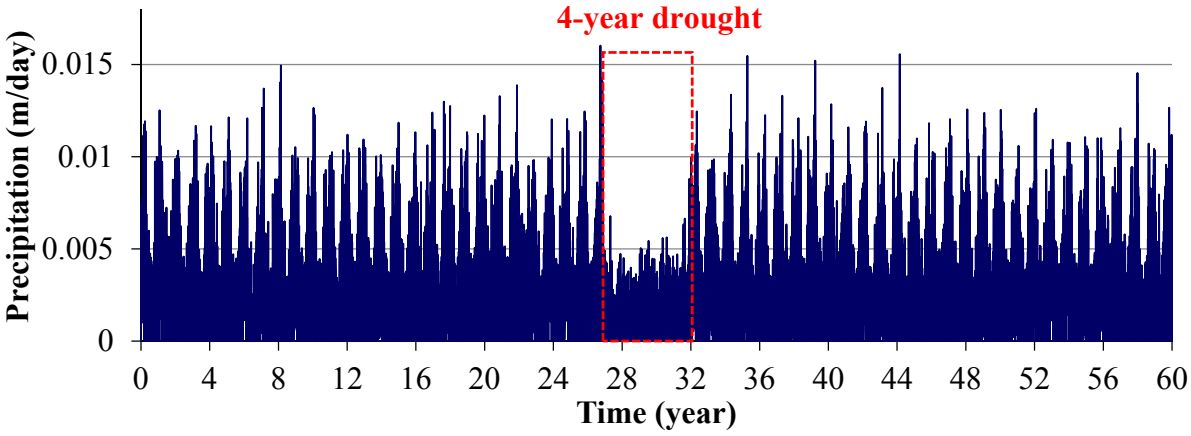

Figure 6. *Cont.*

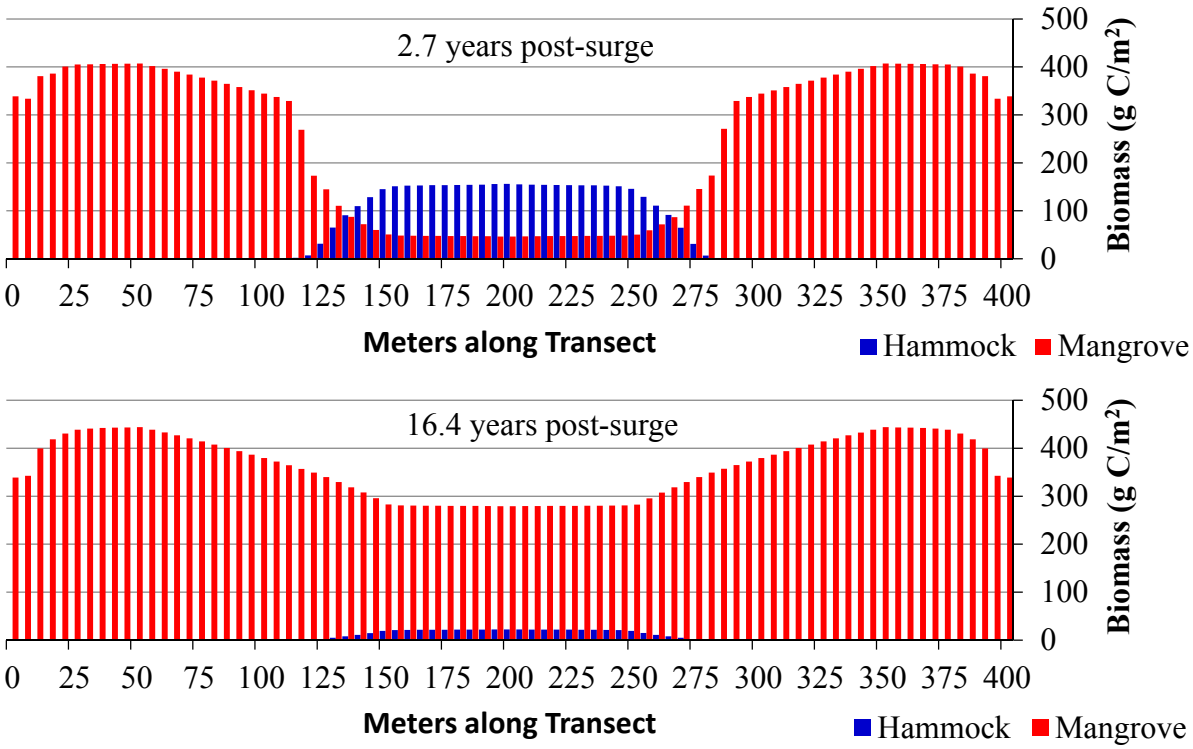

Figure 6. (**Top**) Depiction of precipitation over time used in the scenario, with four-year drought. (**Middle**) Simulated distribution of mangrove (red) and hardwood hammock (blue) vegetation 2.7 years (1000 days) after the storm surge, which occurs at 27.3 years into the simulation. (**Bottom**) Simulated distribution of mangrove (red) vegetation 16.4 years (6000 days) after the storm surge.

3.3. Scenario 4: Gradual SLR

Figure 7 illustrates Scenario 4, of SLR effect on the vegetation distribution at the Coot Bay Hammock transect. We consider here only the effects of sea level rise and ignore any possible effects of major storm surges. These simulation results indicate the mangroves will encroach into the areas of hardwood hammock, confining the freshwater vegetation to a smaller area. Hardwood hammock would persist on the elevated ridge. Further simulations (results not shown) indicate that the hardwood hammocks appear to persist at the elevated ridge unless the sea level rises to a level where the ridge is frequently inundated; e.g., every 20 years or so, with seawater.

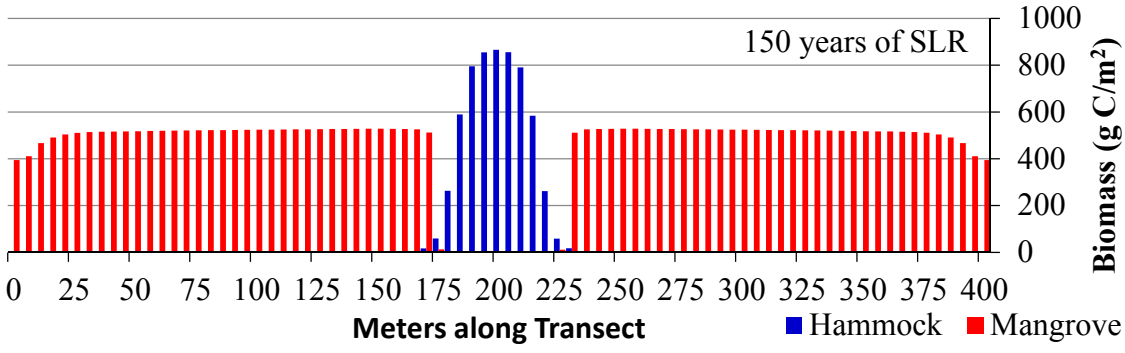

Figure 7. *Cont.*

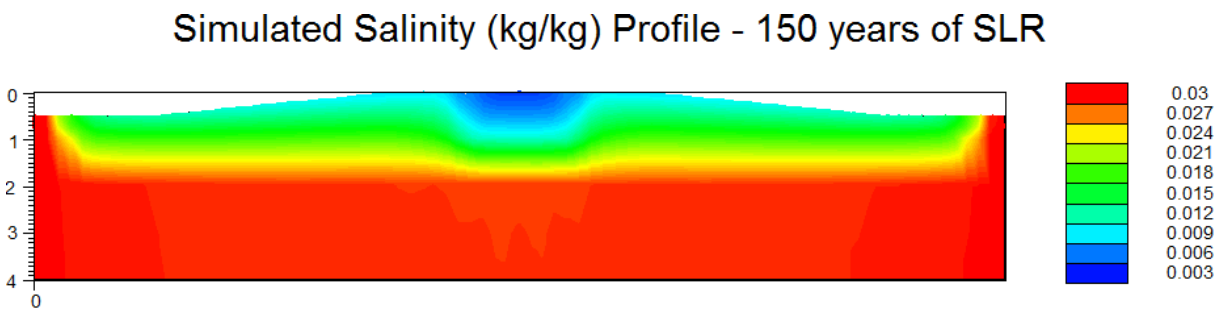

Figure 7. (**Top**) Simulated distribution of mangroves (red) and hardwood hammock (blue) trees along a 400-meter transect across the Coot Bay Hammock after 150 years subject to plausible SLR scenario (3 mm/year). (**Bottom**) Simulated salinity profile.

4. Discussion

Application of MANTRA to the Coot Bay Hammock transect provides insights on the potential vulnerability of the vegetation to storm surges and SLR. Simulations (not shown) that assumed storm surges of about 1 m, but little damage to trees and no prolonged drought did not produce regime shifts of the Coot Bay Hammock to halophytic vegetation. This is consistent with observations in the field showing no recent signs of the start of a shift. The scenarios that we presented that included damage or prolonged drought indicated that a shift might occur under those circumstances. Simulation results for Scenario 2 indicate that mangroves might be able to take over the slightly elevated ridge previously dominated by hardwood hammocks after a storm surge if the surge inflicts heavy damage to the hardwood hammock trees. It is possible that the effects of earlier hurricanes, Hurricane Donna (1960) in particular, may have led to permanent changes over parts of the Coot Bay hammock area. That hurricane produced a 4 m storm surge in the area and destroyed many buttonwood trees, which have not returned. This could be explained by an event like Scenario 2. Precipitation is the source for groundwater lens recharge. Scenario 3, a moderate storm surge followed by a prolonged period of drought, could also cause the shift from hardwood hammocks to mangroves, even though the hardwood hammocks were not badly damaged by the surge.

MANTRA improves greatly over MANHAM on the resolution with which hydrology and salinity are simulated, particularly along the vertical axis. The previous results of MANHAM suggested the possibility of a regime shift from a storm surge [14], but it was cautioned that that it was only a hypothetical result based on simple assumptions of water budget for hydrological dynamics. SUTRA is a highly detailed hydrologic model that has been tested in many contexts and can reliably predict hydrology and solute dynamics if provided good parameter values. Therefore, in MANTRA, the vadose zone is now connected seamlessly with the ground water, rather than the latter being treated as a boundary condition. A freshwater lens emerges naturally above the groundwater in simulations. Importantly, this more realistic treatment of hydrology and salinity dynamics does not change the emergence of sharp boundaries between glycophytic and halophytic vegetation, which was observed in MANHAM [11,14]. This gives us confidence that the self-reinforcing positive feedbacks hypothesized to be acting between each vegetation type and its local soil environment are a reasonable explanation for the sharp ecotone observed, and that these feedbacks may provide resilience to storm surge disturbances that are not too strong. MANTRA shows, like MANHAM, that a storm surge can cause a regime shift,

but it is more conservative, as it shows salinity washing out faster unless there is a drought. So the results of MANTRA show that wind damage to the freshwater vegetation must be severe enough that the mangrove seedlings washed in have a high chance of not being outcompeted by the remaining freshwater vegetation.

Our simulations underscore that three conditions are necessary for a hardwood hammock to undergo a regime shift leading to a mangrove community; sufficiently severe damage to the existing hammock to open a gap to allow growth of invading seedlings, a large input of salinity persisting for a long enough period of time to favor growth of mangrove seedlings in competition remaining freshwater vegetation, and an input of enough mangrove seedlings to allow mangroves to be present in sufficient number to influence the future soil salinity. Surveys of hurricane damage to Everglades hardwood hammocks from Hurricane Andrew (1992) provide an estimate of what a major hurricane can inflict. Studies show heavy damage to 85% of all stems >2 cm diameter and loss of almost all leaves [28,29]. As pointed out in another study [30], the damage provided opportunities for invasive seedlings, which negatively influenced regrowth of the native vegetation. If such damage were inflicted on a coastal hammock, the damage would likely be accompanied by storm surge overwash. Hydrodynamic simulations have been performed of the effects of hurricanes on southern Florida [31]. In particular, those authors performed a hindcast of the "Great Miami Hurricane" of 18 September 1926, including the subsequent meteorological conditions. Simulations of surface water and groundwater salinity in an on shore area showed that salinity levels above 5 g/kg could remain in the soil for close to three years (until July 1929 in their Figure 10), and longer in the upper layer of groundwater. Of course, persistence of soil salinity conditions will vary from location to location with geology and freshwater influxes. However, even short-term exposure to salinity would kill much salinity-intolerant vegetation [32], and the persistence of the high salinity levels for two or three years shown in the modeling of [31] is more than sufficient in MANTRA to favor mangrove seedlings over freshwater vegetation regrowth. Input of mangrove seedlings by storm surges has rarely been studied, but on the basis of one study [33], Jiang *et al.* [34] estimated that up to 2000 propagules per ha could be input from nearby mangrove forest. It has also been suggested that a strategy of mangroves is to constantly produce a large number of seedlings [35] that can be spread by high tides, wind, or animals to provide a "sit-and-wait" seedling bank. Mangrove seedlings and small plants are commonly observed in nearby freshwater areas (*personal observation*).

MANTRA was developed as a tool to study the potential impact of SLR and storm surges on competing halophytic and glycophytic vegetation and, in particular, to investigate the hypothesis that a large input of salinity to a community such as hardwood hammock could result in a regime shift to a halophytic community, such as mangroves. The scenario simulations of MANTRA indicate the feasibility of such shifts, but it can be asked what the evidence is for occurrences in the past. Solid evidence for past regime shifts in southern Florida may be lacking, but that may reflect that up until now there have been few studies focused on vegetation changes following storm surges. A regime shift of vegetation would also take at least a decade to be noticed, and so might appear to be ordinary gradual change rather than an irreversible transition.

Nonetheless, there are some additional examples where regime shifts may be inferred to have occurred in southern Florida. A report on Cape Sable at the southwestern tip of Florida documented the shift in much of this region from freshwater to marine marsh [36]. This shift started to occur suddenly in the 1930s and shows no signs of returning to its original state, so it appears to be an irreversible change,

perhaps a regime shift. It is possible that the Labor Day Hurricane of 1935, which produced a nearly four-meter storm surge over Cape Sable, was at least a partial cause of this shift. As another case, Ross *et al.* (2009) [37], studying vegetation changes in the Florida Keys, noted that "Once sea level reaches a critical level, the transition from a landscape characterized by mesophytic upland forests and freshwater wetlands to one dominated by mangroves can occur suddenly, following a single storm-surge event. We document such a trajectory, unfolding today in the Florida Keys. With sea level projected to rise substantially during the next century, ex-situ actions may be needed to conserve individual species of special concern".

In the Introduction, we noted general evidence from outside of southern Florida that salinity input to a glycophytic community could lead to apparent long-term vegetation shifts [12,13]. In addition, the role of overwash salinity pulses in causing long-term effects on vegetation has been noted in islands of the southern Pacific, where widespread sea flooding by storm surges around the coastlines of South Pacific atolls is a serious hazard during tropical cyclones. For example, in 2005, tropical cyclone Percy inundated the three atolls of Tokelau. The high surge allowed waves to sweep across the low-lying atoll islands. It also inundated the Pukapuka Atoll in the Northern Cook Islands. The immediate effect was on the freshwater lenses that sit on top of saline ground water in these areas [38,39]. Both [38] and [40] stressed that recovery from an overwash event may be prolonged, depending on the amount of seawater that accumulates in the central depression of the atolls. The reason that we extended our original MANHAM model to be combined with SUTRA in MANTRA was to be able to simulate the changes in the freshwater lens and groundwater from storm surges, which could have a long-lasting effect on vegetation.

4.1. Relevance of MANTRA for Management

A goal of the CERP for restoration of the Everglades is to bring additional fresh water south into ENP to restore freshwater habitats. It has been challenging, however, to deliver historic quantities of fresh water sufficient to improve conditions all the way to the coast and Florida Bay, and climate change and SLR will complicate this further [41]. Coastal hardwood communities provide unique habitat for a high diversity of species from plants to mammals [42,43] and protect fresh marsh communities behind them from storm surges. Mangrove migration inland along the west coast, at the expense of hardwood communities and freshwater marsh, has often kept pace with current rates of SLR, although the coastal forests are further stressed by the historic and current reductions of fresh water flow to the Everglades. Along the southern coast, including the study transect of this paper, there is an elevation dip inland of the mangrove/buttonwood/hardwood zone that isolates these hardwood forest communities from simple migration to higher elevations inland, e.g. see [15]. Projections of increasing rates of SLR heighten concerns for maintaining a fresh water hydrologic head that slows salt-water intrusion and allows coastal hardwood communities to have critical time to adapt to changing conditions. MANTRA provides information on how SLR and storm surges may affect vulnerable hardwood hammocks.

4.2. Future Plans

MANTRA development and application is documented in this paper to provide a start in developing a robust model for projecting the effects of overwash and climate change events on groundwater salinity as well as potential changes in vegetation composition. In this paper, the halophytic plant species at Coot

Bay Hammock are generally grouped together as mangroves. However, in fact, there were other halophytic plants that have different dynamics than mangroves along the Coot Bay Hammock transect. Therefore, a better representation of the plant community at Coot Bay can be obtained by including more vegetation types in the model. MANTRA will be improved by revising the plant root network horizontally and vertically, which allows water uptake farther from the main stem and deeper into the ground. Future uses of MANTRA will be extended to a three-dimensional environment.

Precipitation is a major source of groundwater lens recharge. Hence, changes in precipitation pattern will affect groundwater lens recharge and vegetation distribution. Precipitation interception by plant foliage is not modeled explicitly in this model but it should be noted that rainfall interception by plant foliage is an important component in hydrological studies. Zinke [44] reported that interception loss is commonly 10% to 20% in hardwoods. A simulation study assuming this common interception loss will not change the conclusion of this paper.

Based upon the findings of a recent study [45], MANTRA may be revised by using SUTRA-MS to simulate oxygen isotope transport in addition to salt transport, because ^{18}O may be an early indicator of salinity stress on trees. MANTRA shall be applied to study sites along the Waccamaw River, South Carolina, USA. Potential applications to study sites in Malaysia and Mekong River, Vietnam, where floodwaters brought devastating damage to crops like paddy, are also planned. Transitioning to the three-dimensional version of SUTRA will be necessary for some of these projects.

5. Conclusions

The object of this paper was to describe a new model, MANTRA, that combines hydrologic and salinity dynamics based on USGS's SUTRA model, with MANHAM, which models two vegetation types, glycophytic and halophytic, having different transpiration properties with respect to soil salinity. The purpose of the model is to accurately describe effects of SLR and storm surges on the ecotone between these types, given that positive feedbacks between vegetation and soil salinity are important components of this system. The application to Coot Bay Hammock shows consistency with historical data showing that the last major hurricanes, Andrew and Wilma, did not cause a major change (regime shift) of the ecotone, but indicates that larger disturbances, which cause substantial damage to existing vegetation, might have such an effect.

Acknowledgments

S.Y.T. was supported in part by the USGS's Across Trophic Level System Simulation program. Financial support by Grants 305/PMATHS/613418 and 203/PMATHS/6730101 to S.Y.T. and H.L.K. is gratefully acknowledged. M.T. and D.L.D. were supported in part by the USGS's Natural Resources Preservation Project. J.J. was supported in part by National Basic Research Program of China (No. 31200534). Use of trade or product names does not imply endorsement by the U.S. Government. We greatly appreciate the many suggestions and edits of two reviewers for the journal and a USGS reviewer.

Appendix

Appendix 1. Description of MANHAM Model

MANHAM is spatially explicit model of two competing vegetation types, mangroves and hardwood hammocks (though it is adaptable to other competing vegetation types). The vegetation types compete for light and have different tolerances of salinity. The basic assumptions are similar to those in Sternberg *et al*. [11], in which the formation of a sharp boundary between the vegetation types was modeled. Both vegetation types use water from the vadose zone, which overlies a saturated zone of brackish groundwater. Hammock species are assumed to be better competitors in low salinity areas, but cannot grow well under high salinity, where they are out-competed by mangroves. If enough water is withdrawn from the vadose layer by plant water uptake or evaporation, groundwater will infiltrate by capillary action into the vadose layer and increase its salinity. On the other hand, if precipitation exceeds evaporation plus the transpiration of water, then salinity in the vadose layer is percolated towards the underlying ocean water layer and salinity decreases [46]. High vadose zone salinity that develops during Florida's dry season is considered to be the major determinant of vegetation distribution in Florida in this model.

The main mechanism in the model is based on the feedback relationship between the two vegetation types and vadose zone salinity mentioned above. For example, consider a microsite and assume the vadose zone has a particular average salinity during the dry season, which is not sufficiently high to decrease the complete domination of hammock species in an area. During the dry season, as freshwater hammock species continue to transpire water from the vadose layer, ocean water tends to infiltrate and to increase the salinity of the groundwater of the microsite. Because freshwater plants are sensitive to salinity [47], they decrease their transpiration rates, reducing further infiltration of ocean water. In this way the salinity of the vadose layer may be stabilized at low concentrations that are not lethal to freshwater plants. Conversely, consider the alternate equilibrium state where mangroves dominate an area. As mangroves transpire the water in the vadose layer, underlying groundwater with ocean water salinity infiltrates upwards into the vadose zone, but unlike the hammock species, mangroves will continue to transpire and continue to increase the salinity of the vadose layer to levels which would not be tolerated by freshwater hammock species. Thus there will be a tendency for one or the other vegetation type to stabilize itself in a given area, by reinforcing salinity conditions favorable to itself.

This mechanism may explain observations at the landscape level. Our model conceptualizes the landscape as a grid of microsites, or spatial cells, and assumes each grid cell is occupied by a closed canopy of a small number of plants, which can include both mangrove and hammock individuals. Each cell, whether currently dominated by mangrove or hammock species, always contains at least some small fraction of the other type, which can act as 'seeds' for growth under more favorable conditions. Each cell is exposed to precipitation, soil evaporation, tidal deposition of saline water (depending on the cell's elevation in the landscape) and transpiration, which produce vertical fluxes of water in a cell and either increase or decrease the salinity of the vadose zone of that cell. (Evaporation of intercepted water is not considered in this version of the mode). The evapotranspiration depends on the fractions of each of the vegetation types in the cell. The vadose layer of the cell is also assumed coupled to neighboring cells through lateral movement of salinity. The strongest mechanism for this transport may be water uptake

by the roots of plants in the neighboring cells, which redistributes water and salinity between cells. Thus there is some tendency for adjacent cells to approach over time the same vadose zone salinity, allowing the possibility for each vegetation type to spread horizontally from one cell to dominate adjacent cells.

We hypothesize that a model landscape of mangrove and hardwood hammock trees, initially randomly mixed and then subjected to these abiotic factors, will self-organize into a pattern similar to those observed in nature, having strong aggregation into areas of either solid hammock or mangrove vegetation (vegetation clumping), such that there can be rapid changes between the vegetation types along gradual clines in microtopography. However, we also hypothesize that a large enough disturbance can change this pattern. For example, a storm surge that deposits a large amount of saline water across the landscape may cause hammock trees to slow their growth sufficiently to be outcompeted by mangroves over a sufficiently long time period to allow mangroves take over. Thus a large area may "switch" vegetation type quickly.

This model was implemented quantitatively as a two-dimensional grid of square spatial cells, where the sides of each cell were assumed to be in the range of a few to several meters.

Hydrology and salinity: The salinity in a given spatial cell is determined first of all by the difference between the precipitation, P, which brings in fresh water to the top of the vadose zone, and the evaporation, E, and plant uptake of water, R. This difference is called the infiltration rate, I_{NF};

$$I_{NF} = E + R - P \text{ (mm day}^{-1}\text{)} \tag{A1.1}$$

and the dynamics of salinity in the vadose zone are given by the equations

$$nz\frac{dS_V}{dt} = I_{NF}S_{wt} \text{ for } I_{NF} > 0 \tag{A1.2}$$

$$\varepsilon z\frac{dS_V}{dt} = I_{NF}S_V \text{ for } I_{NF} < 0 \tag{A1.3}$$

where z (mm) is the depth of the vadose zone of a given cell, ε is the porosity, and S_V and S_{wt} are the salinities of the pore water in the vadose zone and of the underlying saline groundwater, respectively. Positive values of infiltration (A1.2) occur when precipitation is less than the water demanded by evaporation and transpiration; then water from the underlying saline groundwater infiltrates upward into the vadose zone. Note that when $I_{NF} > 0$, salt is deposited in the vadose zone by evapotranspiring water, so concentrations can build up to high levels. Negative values occur when precipitation exceeds evaporation and transpiration demands; then water percolates downward into the underlying groundwater table.

The assumption of a groundwater table with fixed salinity is a useful first approximation, but it is also possible that the salinity dynamics of at least the surface layer of groundwater is more complex. The effect of an upper layer of groundwater that is affected both by precipitation and flow of groundwater from higher elevations is examined in an appendix (see on-line Appendix 2), while here we restrict ourselves to examining the model with the simpler assumption.

Evaporation was assumed to be small compared with transpiration and was neglected, since we are assuming a dense canopy in each cell, which inhibits evaporation. Moreira, *et al.* [48] and Harwood, *et al.* [49] both observed that in forests transpiration dominates as the vapor generator compared to evaporation. R_{TOTAL} depends on the transpiration and gross productivity of each vegetation

type in the spatial cell (see A1.13 below). The maximum possible water uptake rate by freshwater hammocks is assumed to be 2.6 mm/d. This value is based on previous studies indicating that transpiration in tropical forests lies within this range [38]. Uptake of water as a function of salinity by the hardwood hammock $R_1(S_v)$ and mangrove species $R_2(S_v)$ is given by the respective empirical relations (Figure 2):

$$R_1(S_v) = 2.6\left(1 - \frac{S_v}{3.14 + S_v}\right) \text{ mm day}^{-1} \quad \text{(A1.4a)}$$

$$R_2(S_v) = 4.4\left(\frac{100 - S_v}{15 + 100 - S_v}\right) \text{ mm day}^{-1} \quad \text{(A1.4b)}$$

in which hammocks reduce their transpiration by ½ when the salinity of the pore water is 3.14 ppt, while mangrove transpiration is not reduced by ½ until the salinity of the pore water is 85 ppt.

In addition to the above hydrologic processes, tidal effects were imposed on all spatial cells at elevations low enough to be affected. The effect of tides on the salinity of spatial cells was calculated as follows. On each day a single high tide was assumed. The height of the tide above the surface of each spatial cell was generated as a function of the mean and a randomly generated variation within the observed limits of tidal flux of the empirical data, so that the number of spatial cells covered by the tide on a given day varied in number. The amount of salt contained in the volume of water above the cell, assumed to have a salinity of 30 ppt, was allowed to mix homogeneously with the vadose zone below. In all model simulations precipitation and effects of tides were prescribed on a daily basis. Means and standard deviations of daily precipitation (NOAA, National Weather Services Forecast Office, Florida) and daily tidal height (NOAA, Tide & Current Historic data base, Key West Station) for each month were derived from 162 and 5 years of empirical data respectively. Daily values were determined using a normal random number generator, with values truncated at zero.

We assume there is also horizontal diffusion of salinity between cells. We used a diffusion constant of $D = 0.0005$, which is about seven times the theoretical value used by Passioura, *et al.* [50] and ten times the laboratory values of [51]. However, we assume that classical diffusion is not the only process causing mixing of solute between cells. The extension of roots across cell boundaries can contribute to the mixing among cells, and we believe our value is reasonable.

Vegetation dynamics: A given cell could be occupied by the two types of vegetation simultaneously, and, in fact, even in cells dominated by one type, small amounts of the other type tended to persist. The biomasses of each species in a given spatial cell were explicitly modeled, as well as the mechanism of competitive dominance of the hammock vegetation over mangrove vegetation under very low soil salinity conditions. We used an approach similar to that of Herbert, *et al.* [52] for competition between species of different functional types, with a slight difference. This is explained in detail in Teh *et al*. [14] and Herbert, *et al.* [52]. Herbert *et al.* [52] assumed that the plant types differed in their abilities to compete for light and nutrients. Here we assumed that the plants differed only in their ability to compete for light, with the additional assumption that the hardwood species were superior in low salinity. We assumed that in any particular microsite the equations for the different vegetation types (hardwood hammock and mangrove in this case) were

$$\frac{dB_{Ci}}{dt} = U_{Cvi} - M_{Cvi} - L_{Cvi} \ (i = 1,2) \tag{A1.5}$$

where B_{ci} is carbon in plant biomass (gCm^{-2}), U_{Cvi} is gross productivity ($gCm^{-2}day^{-1}$),

$$U_{Cvi} = \frac{Q(S_v) g_{Ci} w_{Ci} I(1 - e^{-k_l S_{CT}})}{w_{C1} + w_{C2}} \ (i = 1,2) \tag{A1.6}$$

where w_{C1} and w_{C2} incorporate competition for light, depending on how much of the canopy of a spatial cell each occupies (see Herbert *et al.* [52] for details);

$$w_{Ci} = \frac{2(1 - e^{-k_l S_{Ci}})}{(1 + e^{-k_l S_{Ci}})} \prod_{j=1}^{2} \left(\frac{f_{Cj} e^{-k_l S_{Ci}} + f_{Ci}}{f_{Ci} + f_{Cj}} \right) \ (i = 1,2) \tag{A1.7}$$

where the $f_{Ci} = 0.58/c_{ii}$ parameters are measures of canopy dominance (e.g., the relative degree to which trees of one species shade another due to height differentials). S_{Ci} (m^2 m^{-2}) is the leaf area index of species i in a spatial cell,

$$S_{Ci} = b_{Ci} B_{Ai} \ (i = 1,2) \tag{A1.8}$$

B_{Ai} (gCm^{-2}) is active tissue carbon of each plant species,

$$B_{Ai} = \frac{c_{ii} B_{A\max,i} B_{Ci}}{B_{A\max,i} + c_{1i} B_{C1} + c_{2i} B_{C2}} \tag{A1.9}$$

where the parameters c_{ij} are allometric parameters governing the amount of energy allocated to active tissue (leaves). Note that the biomass of species j can affect the allocation of biomass of species i. We assumed the effect of salinity on productivity of species i, $Q_i(S_v)$, occurs through its effect on the water uptake rate, normalized by the maximum possible rate;

$$Q_i(S_v) = \frac{R_i(S_v)}{R_i(0)} \ (i = 1,2) \tag{A1.10}$$

M_{Cvi} (g C m^{-2} day^{-1}) is the respiration of each plant;

$$M_{Cvi} = m_{Ai} B_{Ai} + m_{wi}(B_{Ci} - B_{Ai}) \ (i = 1,2) \tag{A1.11}$$

where the rates differ between dead and living matter. L_{Cvi} (g C m^{-2} day^{-1}) is litterfall of each plant,

$$L_{Cvi} = l_{Ai} B_{Ai} + l_{wi}(B_{Ci} - B_{Ai}) \ (i = 1,2) \tag{A1.12}$$

Total evapotranspiration from a cell is linearly related to the evapotranspiration of each species, multiplied by its fraction of the primary production in that spatial cell;

$$R_{TOTAL} = \frac{U_{Cv1}}{U_{Cv1} + U_{Cv2}} R_1 + \frac{U_{Cv2}}{U_{Cv1} + U_{Cv2}} R_2 \tag{A1.13}$$

We do not have parameter values related to light competition for these vegetation types, but made estimates that allowed hardwood hammock vegetation to dominate for salinities below 7 ppt.

To improve the fit of the model to the boundary between hardwood hammocks and mangroves of the Coot Bay Hammock, some moderate modifications were made to the original MANHAM formulation and the parameter value. Notably, we varied the light extinction coefficients, k_i, for the two species, as well as the parameters and equation for leaf area index of each species i in a spatial cell. We gave the hardwood hammock an advantage in light use shading out of the mangroves, which would allow hardwood hammock to outcompete the mangroves at lower salinity areas. The equation for leaf area index, Sc_i , of species i in a spatial cell is revised from

$$Sc_i = bc_i B_{Ai} \tag{A1.14a}$$

(where bc_i is the leaf area index per unit active tissue and B_{Ai} is the active tissue carbon, see Equation (8) in Teh *et al*. [14]) to Equation (A1.14b) below to include the plant water uptake effort $Q_i(C)$, following Herbert *et al*. [52].

$$Sc_i = bc_i B_{Ai} \cdot Q_i\left(C\right) \tag{1}$$

where C = solute concentration [M_s/M_f]. The changes to (A1.14a) would cause the hardwood hammocks to diminish in biomass quickly at higher salinities, as the water uptake effort $Q_i(S_v)$ is less than halved when the salinity is higher than 3.14 ppt. The revised formulation (A1.14b) alone results in a situation where the mangroves outcompete the hardwood hammocks at the elevated ridge, which also is not realistic. However, the increase of light extinction factor k_i for hardwood hammocks ensures that hardwood hammocks outcompete the mangroves at lower salinities. These revisions allow the mangrove and hardwood hammocks to evolve, in a more realistic manner, into the distribution observed at Rowdy Bend.

Appendix 2. MANTRA Version 1 Manual: August 1, 2014

This report briefly describes the coupled hydrology-salinity-vegetation model, MANTRA, for analysis of the feedback effect of competing glycophytes (hardwood hammocks) and halophytes (mangroves) on the groundwater flow and salinity regime. MANTRA can be further revised to include more competing plants [15] by incorporating the dynamics of these plants in the MANHAM module. MANTRA was developed by integrating the USGS spatially explicit models of vegetation community dynamics along coastal salinity gradients (MANHAM) into the USGS groundwater models (SUTRA). Table A2.1 lists the files needed to run MANTRA. The MANHAM [11,14] module is incorporated into SUTRA [16] in sutra_2_2.f by accounting for the exchange of fluid and solute mass between the models. A storm surge event is incorporated into usubs_2_2.f as time-dependent specified pressure.

In MANTRA, the total amount of water required for plant transpiration is subtracted from the SUTRA cells covered by plants. The fluid mass source/sink term Q_{IN}, originally available in SUTRA, is used to characterize the uptake of water by plant [18–20]. This source/sink term accounts for external addition/subtraction of fluid including pure water mass plus the mass of any solute dissolved in the source fluid. This fluid uptake by plant reduces the fluid mass in the cells, which in turn increases the solute (salt) concentration. Plant growth in MANHAM depends on the actual fluid available in the cells for transpiration and the solute concentration. Units are presented in square brackets [ ] with M being the unit of mass, L the unit of length and s the unit of time in seconds. The relations are formulated for

simulations of a 2D cross-sectional fishnet domain with saturated-unsaturated, variable-density (pressure) with single species (solute) transport. It is assumed at present that the plants will only withdraw water from the uppermost layer of cells/nodes and that the plant roots cover the entire surface area of the cells (Figure A2.1). Currently, the vegetation and groundwater modules operate at the same time step. This is expected to slow down the computation, particularly when there are large numbers of element. As the hydrological processes and vegetation dynamics operate at different time scale, a method similar to those employed in the SEHM model by Jiang, *et al.* [53] can be employed to optimize the computation time.

Table A2.1. List of files needed to run MANTRA.

Filename	Remarks
SUTRA.FIL	These are the files that are also needed to run the original version of SUTRA.
SUTRA.inp	These files contain the input parameters for the groundwater flow and solute
SUTRA.ics	transport simulation. These files can be created by using ArgusONE.
MANTRA.exe	This is the executable file of MANTRA. This executable file is built from fmods_2_2.f, sutra_2_2.f, ssubs_2_2.f, usubs_2_2.f. Modifications have been made to incorporate the MANHAM module into sutra_2_2.f. A storm surge event is incorporated into usub_2_2.f as time-dependent specified pressure.
MANHAM.DAT	This is the input file for the MANHAM module in MANTRA. This file contains the input parameters related to the vegetation.

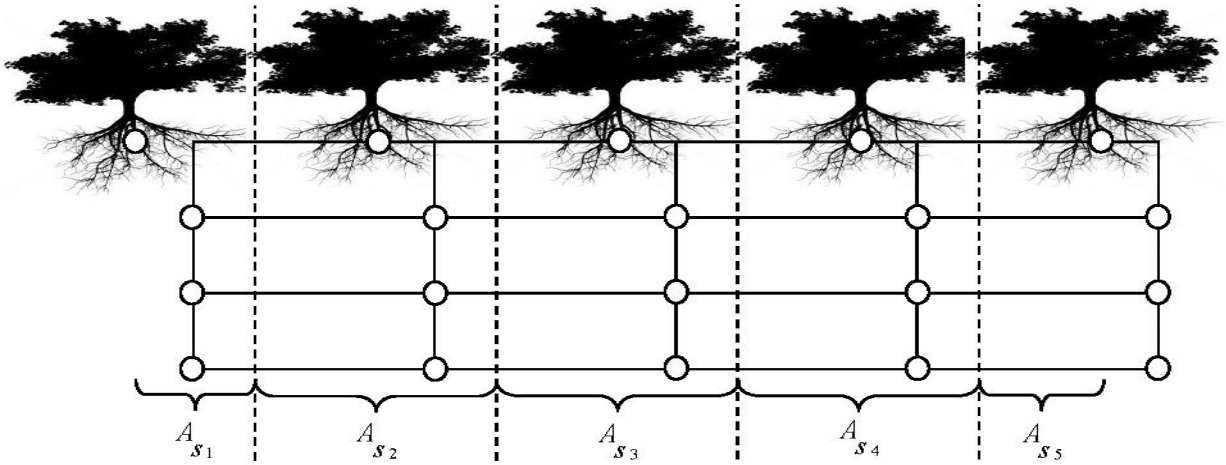

Figure A2.1. Schematic sketch of a simulation case. A_{s_i} = Surface area for node *i* at uppermost layer of cells.

The uptake of water as a function of salinity for hardwood hammock (R_1) and mangrove (R_2) are estimated by the empirical relations Equations (A2.1) and (A2.2).

$$R_1(C) = R_{\max,1}\left(1 - \frac{C}{S_{half,1} + C}\right) \quad [\text{L/s}] \tag{A2.1}$$

$$R_2(C) = R_{\max,2}\left(\frac{0.1-C}{S_{half,2}+0.1-C}\right) \text{ [L/s]} \tag{A2.2}$$

with C = solute concentration [M_s/M_f] calculated by SUTRA. Here, Fluid mass per unit time (Q_p) required by the plants in a certain cell is then estimated by (A2.3).

$$Q_p = (R_1 + R_2)\cdot A_s \cdot \rho \text{ [M/s]} \tag{A2.3}$$

Here, Q_p = fluid mass per unit time extracted in a certain cell for plant transpiration [M/s]; A_s = cell surface area [L^2]; ρ = fluid density [M/L^3]. For cross-sectional model, the width of each cell is assumed to be 1.0. Thus, the cell surface area depends mainly on the length or horizontal grid size (Figure A2.1). The actual fluid mass being subtracted from a cell due to evapotranspiration depends on the saturation S_w and porosity ε in the cell, leading to Equation (A2.4).

$$Q_{IN} = -Q_p \cdot \varepsilon \cdot S_w \text{ [M/s]} \tag{A2.4}$$

Here, Q_{IN} = total mass sink (due to plant transpiration) [M/s]; ε = porosity [V_v/V]; S_w = water saturation [V_w/V_v] with V = total volume, V_v = volume of voids, V_w = volume of water. Suppose porosity ε is kept constant at 1.0. When the void space is completely filled with fluid and is said to be saturated, that is $S_w = 1$, the actual water uptake by plant will be equivalent to the amount of water required by the plants Q_p. When the void space is only partly water filled and is referred to as being unsaturated, that is $S_w < 1$, the actual water uptake by plant will decrease as a factor of the saturation S_w. Similar to transpiration, precipitation is implemented as a source term in MANTRA. The precipitation rate is varied stochastically on daily basis. Daily values are determined using a normal random number generator, with values truncated at zero.

Since the storm surge event is incorporated into usubs_2_2.f as time-dependent specified pressure, time-dependent specified pressure for the surface nodes should be indicated in the SUTRA input file (sutra.inp) so that the usubs_2_2.f routine will be called for implementation. The storm surge event is simulated by allowing the surface nodes to be inundated with seawater of certain depth and salinity. This form of inundation will change the hydrostatic pressure at the surface nodes. Equations (A2.5) and (A2.6) [21] are respectively used to specify the pressure and concentration at surface nodes inundated by seawater during a storm surge event.

$$p = \rho_{sea} \cdot g \cdot (h_{surge} - y) \text{ [M/(L·s}^2\text{)]} \tag{A2.5}$$

$$C = S_{sea} \text{ [M}_s\text{/M}_f\text{]} \tag{A2.6}$$

Here, p = pressure at top layer nodes [$M/(L\cdot s^2)$], ρ_{sea} = fluid density of seawater [M/L^3], h_{surge} = inundation depth [L], y = node height [L], and S_{sea} = seawater salinity [M_s/M_f]. Figure A2.2 shows an example of input file (MANHAM.DAT) for MANHAM module in MANTRA for the example case of Rowdy Bend. Table A2.2 summarizes the list of parameters in MANHAM.DAT with their description, type, value and unit.

Table A2.2. List of parameters in MANHAM.DAT with their description, type, value and unit.

Variable Name		Type	Description	Value	Unit
Input File	**Eqn**				
SUTRA Node Control					
NSNODE	–	Integer, I10	Number of sets of surface nodes	1	–
NFIRST	–	Integer, I10	First surface node number in SUTRA domain	1	–
NLAST	–	Integer, I10	Last surface node number in SUTRA domain	1601	–
NDIFF	–	Integer, I10	Interval between surface node numbers	20	–
Storm Surge Control					
IT_Surge	–	Integer, I10	Iteration time of a storm surge event	60,000	–
SDepth	h_{surge}	Real, F10.2	Storm surge inundation depth in relation to the height of SUTRA computational domain	10.5	m
SSalinity	S_{sea}	Real, F10.3	Storm surge water salinity	0.030	kg/kg
Plant Initial Condition (IC) Control					
NSPEC	–	Integer, I10	Number of plant species	2	–
NRAND	–	Integer, I10	Seed for random number generator	1234	–
BEGINHAM	–	Real, F10.2	Ratio of cells dominated by hardwood hammock	0.50	–
BC0	–	Real, F10.2	Total initial biomass in a cell	20,000.00	g C m^{-2}
PERSPEC	–	Real, F10.2	Ratio of plant *i* in a cell	0.50	–

Table A2.2. *Cont.*

Variable Name		Type	Description	Value			Unit
Input File	**Eqn**						
Light Parameters							
SI	I	Real, F10.3	Solar irradiance	0.010			GJ $m^{-2}day^{-1}$
EKI	k_i	Real, F10.4	Light extinction factor	0.600	0.400		
GC(NSPEC)	g_{Ci}	Real, F10.1	Light-use efficiency	520.0	380.0		g C GJ^{-1}
BAMAX(NSPEC)	$B_{Amax,i}$	Real, F10.1	Maximum value attainable by B_{Ai}	350.0	350.0		g C m^{-2}
Plant Parameters							
bc(NSPEC)	b_{ci}	Real, F10.4	Leaf area per unit carbon	0.0355	0.0170		m^2/g C
RA(NSPEC)	r_{Ai}	Real, F10.4	Active tissue respiration rate	4.0000	4.0000		$year^{-1}$
RW(NSPEC)	r_{Wi}	Real, F10.4	Woody tissue respiration rate	0.0296	0.0296		$year^{-1}$
RMA(NSPEC)	m_{Ai}	Real, F10.4	Active tissue litter loss rate	1.7000	1.7000		$year^{-1}$
RMW(NSPEC)	m_{Wi}	Real, F10.4	Woody tissue litter loss rate	0.0148	0.0148		$year^{-1}$
RFWMAX(NSPEC)	$R_{max,i}$	Real, F10.4	Maximum water uptake for plant NSPEC	0.0026	0.0088		mm day^{-1}
SATK(NSPEC)	$S_{half,i}$	Real, F10.4	Half saturation constant for maximum water uptake for plant NSPEC	3.1400	15.0000		ppt
C(NSPEC, NSPEC)	c_{ii}	Real, F10.4	Parameters for plant allometry	0.1000 0.5000	0.1000 0.5000		–
Environmental Parameters							
VPRE(12)	M_{pre}	Real, F10.4	Means precipitation rate for twelve months	1.590	1.360	...	mm day^{-1}
VPRESD(12)	SD_{pre}	Real, F10.4	Standard deviations of precipitation rate	1.870	1.200	...	mm day^{-1}

```
  INPUT FILE FOR MANHAM

----+----+----+----+----+----+----+----+----+----+----+----+----+----+----+
    SUTRA Node Control
----+----+----+----+----+----+----+----+----+----+----+----+----+----+----+
  NSNODE                    1
  NFIRST                    1
  NLAST                  1601
  NDIFF                    20

----+----+----+----+----+----+----+----+----+----+----+----+----+----+----+
    Storm Surge Control
----+----+----+----+----+----+----+----+----+----+----+----+----+----+----+
  IT_Surge               60000
  SDepth                  10.5
  SSalinity              0.030

----+----+----+----+----+----+----+----+----+----+----+----+----+----+----+
    Plant IC Control
----+----+----+----+----+----+----+----+----+----+----+----+----+----+----+
  NSPEC                     2
  NRAND                  1234
  BEGINHAM                0.50
  BC0                 20000.00
  PERSPEC                 0.50

----+----+----+----+----+----+----+----+----+----+----+----+----+----+----+
    Light Parameters
----+----+----+----+----+----+----+----+----+----+----+----+----+----+----+
  SI                     0.010
  EKI                    0.600     0.400
  GC(NSPEC)              520.0     380.0
  BAMAX(NSPEC)           350.0     350.0

----+----+----+----+----+----+----+----+----+----+----+----+----+----+----+
    Plant Parameters
----+----+----+----+----+----+----+----+----+----+----+----+----+----+----+
  bc(NSPEC)             0.0355    0.0170
  RA(NSPEC)             4.0000    4.0000
  RW(NSPEC)             0.0296    0.0296
  RMA(NSPEC)            1.7000    1.7000
  RMW(NSPEC)            0.0148    0.0148
  RFWMAX(NSPEC)         0.0026    0.0088
  SATK(NSPEC)           3.1400   15.0000
  C(NSPEC,NSPEC)        0.1000    0.1000
                        0.5000    0.5000  ( C11,C21,C12,C22)

----+----+----+----+----+----+----+----+----+----+----+----+----+----+----+
    Environmental Parameters
----+----+----+----+----+----+----+----+----+----+----+----+----+----+----
+----+----+----+----+----+----+----+----+----+----+----+----+----+
  VPRE(12)          1.590     1.360     1.320     1.500     2.730     3.820
                    3.090     4.050     5.480     4.640     2.020     1.570
  VPRESD(12)        1.870     1.200     1.290     1.800     2.220     2.710
                    1.970     2.130     2.710     3.470     2.840     1.520
```

Figure A2.2. Example input file (MANHAM.DAT) for MANHAM module in MANTRA for the example case of Rowdy Bend.

References

1. Nicholls, R.J.; Cazenave, A. Sea-level rise and its impact on coastal zones. *Science* **2010**, *328*, 1517–1520.
2. Gornitz, V. *Rising Seas: Past, Present, Future*; Columbia University Press: New York, NY, USA, 2013; p. 344.
3. Anderson, W.P., Jr. Aquifer salinization from storm overwash. *J. Coast. Res.* **2002**, *18*, 413–420.
4. Anderson, W.P., Jr.; Lauer, R.M. The role of overwash in the evolution of mixing zone morphology within barrier islands. *Hydrogeol. J.* **2008**, *16*, 1483–1495.
5. Terry, J.P.; Falkland, A.C. Responses of atoll freshwater lenses to storm-surge overwash in the Northern Cook Islands. *Hydrogeol. J.* **2010**, *18*, 749–759.
6. Sklar, F.H.; Chimney, M.J.; Newman, S.; McCormick, P.; Gawlik, D.; Miao, S.; McVoy, C.; Said, W.; Newman, J.; Coronado, C. The ecological-societal underpinnings of Everglades restoration. *Front. Ecol. Environ.* **2005**, *3*, 161–169.
7. Ross, M.S.; O'Brien, J.J.; Flynn, L.J. Ecological site classification of Florida Keys terrestrial habitats. *Biotropica* **1992**, *24*, 488–502.
8. Smith, T.J.I.; Foster, A.M.; Tiling-Range, G.; Jones, J.W. Dynamics of mangrove–marsh ecotones in subtropical coastal wetlands: fire, sea-level rise, and water levels. *Fire Ecol.* **2013**, *9*, 66–77.

9. Gosz, J.R. Ecotone hierarchies. *Ecol. Appl.* **1993**, 3, 369–376.
10. Snyder, J.R.; Herndon, A.; Robertson, W.B.J. South Florida rockland. In *Ecosystems of Florida*; Myers, R.L., Ewel, J.J., Eds.; The University of Central Florida Press: Orlando, FL, USA, 1990; pp. 230–279.
11. Sternberg, L.D.L.; Teh, S.Y.; Ewe, S.M.L.; Miralles-Wilhelm, F.; DeAngelis, D.L. Competition between hardwood hammocks and mangroves. *Ecosystems* **2007**, *10*, 648–660.
12. Baldwin, A.H.; Mendelssohn, I.A. Effects of salinity and water level on coastal marshes: An experimental test of disturbance as a catalyst for vegetation change. *Aquatic Botany* **1998**, *61*, 255–268.
13. Steyer, G.D.; Cretini, K.F.; Piazza, S.; Sharp, L.A.; Snedden, G.A.; Sapkota, S. *Hurricane Influences on Vegetation Community Change in Coastal Louisiana*; U.S. Geological Survey: Reston, VA, USA, 2010.
14. Teh, S.Y.; DeAngelis, D.L.; Sternberg, L.D.L.; Miralles-Wilhelm, F.R.; Smith, T.J.I.; Koh, H.L. A simulation model for projecting changes in salinity concentrations and species dominance in the coastal margin habitats of the Everglades. *Ecol. Model.* **2008**, *213*, 245–256.
15. Saha, A.; Saha, S.; Sadle, J.; Jiang, J.; Ross, M.; Price, R.; Sternberg, L.; Wendelberger, K. Sea level rise and South Florida coastal forests. *Clim. Chang.* **2011**, *107*, 81–108.
16. Voss, C.I.; Provost, A.M. *SUTRA, A Model for Saturated-Unsaturated Variable-Density Ground-Water Flow with Solute or Energy Transport*; U.S. Geological Survey Water-Resources Investigations Report 02–4231; U.S. Geological Survey: Reston, VA, USA, 2010; p. 291.
17. Voss, C. USGS SUTRA code—History, practical use, and application in Hawaii. In *Seawater Intrusion in Coastal Aquifers—Concepts, Methods and Practices*; Practices, J., Bear, A., Cheng, H.D., Sorek, S., Ouazar, D., Herrera, I., Eds.; Kluwer Acdemic Publishers: Dordrecht, Netherlands 1999; pp. 249–313.
18. Vrugt, J.; Wijk, M.V.; Hopmans, J.W.; Šimunek, J. One-, two-, and three-dimensional root water uptake functions for transient modeling. *Water Resour. Res.* **2001**, *37*, 2457–2470.
19. Zhu, Y.; Ren, L.; Skaggs, T.H.; Lü, H.; Yu, Z.; Wu, Y.; Fang, X. Simulation of Populus euphratica root uptake of groundwater in an arid woodland of the Ejina Basin, China. *Hydrol. Process.* **2009**, *23*, 2460–2469.
20. Tian, W.; Li, X.; Wang, X.-S.; Hu, B. Coupling a groundwater model with a land surface model to improve water and energy cycle simulation. *Hydrol. Earth Syst. Sci. Discuss.* **2012**, *9*, 1163–1205.
21. Kooi, H.; Groen, J.; Leijnse, A. Modes of seawater intrusion during transgressions. *Water Resour. Res.* **2000**, *36*, 3581–3589.
22. Saha, A.; Moses, C.; Price, R.; Engel, V.; Smith, T., III; Anderson, G. A hydrological budget (2002–2008) for a large subtropical wetland ecosystem indicates marine groundwater discharge accompanies diminished freshwater flow. *Estuaries Coasts* **2012**, *35*, 459–474.
23. Light, S.S.; Dineen, J.W. Water control in the Everglades: A historical perspective. In *Everglades: The Ecosystem and its Restoration*, Davis, S.M., Ogden, J.C., Eds.; St. Lucie Press: Florida, FL, USA, 1994; pp. 47–84.
24. Sadle, J. Everglades National Park. Homestead, Florida, FL, USA. Personal communication, 2014.

25. Olmstead, I.C.; Loope, L.L. Vegetation along a Microtopographic Gradient in the Estuarine Region of Everglades National Park, Florida, USA; South Florida Research Center: Florida, FL, USA, 1981; p. 41.
26. Smith, T.; Anderson, G.H.; Tiling, G. *Science and the Storms: The USGS Response to the Hurricanes of 2005*; Farris, G.S., Smith, G.J., Crane, M.P., Demas, C.R., Robbins, L.L., Lavoie, D.L., Eds.; U. S. Geological Survey Circular 1306: Reston, VA, USA, 2007; pp. 169–174.
27. Wanless, H.R.; Parkinson, R.W.; Tedesco, L.P. Sea level control on stability of Everglades wetlands. In *Everglades: The Ecosystem and Its Restoration*; St. Lucie Press: Delray Beach, FL, USA, 1994, pp. 199–223.
28. Armentano, T.V.; Doren, R.F.; Platt, W.J.; Mullins, T. Effects of Hurricane Andrew on coastal and interior forests of southern Florida: Overview and synthesis. *J. Coast. Res.* **1995**, *21*, 111–144.
29. Slater, H.H.; Platt, W.J.; Baker, D.B.; Johnson, H.A. Effects of Hurricane Andrew on damage and mortality of trees in subtropical hardwood hammocks of Long Pine Key, Everglades National Park, Florida, USA. *J. Coast. Res.* **1995**, *21*, 197–207.
30. Horvitz, C.C.; Pascarella, J.B.; McMann; S.; Freedman, A.; Hofstetter, R.H. Functional roles of invasive non-indigenous plants in hurricane-affected subtropical hardwood forests. *Ecol. Appl.* **1998**, *8*, 947–974.
31. Swain, E.D.; Krohn, D.; Langtimm, C.A. Numerical computation of hurricane effects on historic coastal hydrology in southern Florida. *Ecol. Process.* **2015**, *4*, 4, doi:10.1186/s13717-014-0028-3.
32. Hook, D.D.; Buford, M.A.; Williams, T.M. Impact of Hurricane Hugo on the South Carolina coastal plain forest. *J. Coast. Res.* **1991**, *8*, 291–300.
33. Rathcke, B.J.; Landry, C.L. Dispersal and recruitment of white mangrove on San Salvador Island, Bahamas after Hurricane Floyd. In Proceedings of the Ninth Symposium on the Natural History of the Bahamas, San Salvador, Bahamas, 14–18 June 2001.
34. Jiang, J.; DeAngelis, D.L.; Anderson, G.H.; Smith, T.J., III. Analysis and simulation of propagule dispersal and salinity intrusion from storm surge on the movement of a marsh-mangrove ecotone in South Florida. *Estuar. Coasts* **2014**, *37*, 24–35.
35. López-Hoffman, L.; Ackerly, D.D.; Anten, N.P.R.; Denoyer, J.L.; Martinez-Ramos, M. Gap-dependence in mangrove life-history strategies: A consideration of the entire life cycle and patch dynamics. *J. Ecol.* **2007**, *95*, 1222–1233.
36. Wanless, H.R.; Brigitte, M.V. *Coastal Landscape and Channel Evolution Affecting Critical Habitats at Cape Sable*; Final Report to ENP; Everglades National Park: Homestead, FL, USA, 2005.
37. Ross, M.S.; O'Brien J.J.; Ford, R.G.; Zhang, K.; Morkill, A. Disturbance and the rising tide: The challenge of biodiversity management for low island ecosystems. *Front. Ecol. Environ.* **2009**, *9*, 471–478.
38. Cabral, O.M.; McWilliam, A.; Roberts, J. In-canopy microclimate of Amazonian forest and estimates of transpiration. In *Amazon Deforestation and Climate*; Gash, J.; Nobre, C.; Roberts, J.; Victoria, R., Eds; Wiley Press: Chichester, UK, 1996; pp. 207–220.
39. White, I.; Falkland, T. Management of freshwater lenses on small Pacific islands. *Hydrogeol. J.* **2010**, *18*, 227–246.

40. Chui, T.F.; Terry, J.P. Modeling fresh water lens damage and recovery on atolls after storm-wave washover. *Ground Water* **2012**, *50*, 412–420, doi:10.1111/j.1745–6584.2011.00860.x.
41. Pearlstine, L.G.; Pearlstine, E.V.; Aumen, N.G. A review of the ecological consequences and management implications of climate change for the Everglades. *J. Am. Benthol. Soc.* **2010**, *29*, 1510–1526.
42. Odum, W.E.; McIvor, C.C.; Smith, T.J., III. *The Ecology of the Mangroves of South Florida: A Community Profile*; Bureau of Land Management Fish and Wildlife Service: Washington, DC, USA, 1982.
43. Meshaka, W.; Loftus, W.F.; Steiner, T. The herpetofauna of Everglades National Park. *Fla. Sci.* **2000**, *63*, 84–103.
44. Zinke, PJ. Forest interception study in the United States. In *Forest Hydrology*; Sopper, W.E., Lull, H.W., Eds.; Pergamon: Oxford, UK, 1967; pp. 137–161.
45. Zhai, L.; Jiang, J.; DeAngelis, D.L.; Sternberg, L.S.L. Prediction of plant vulnerability to salinity increase in a coastal ecosystem by stable isotopic composition of plant stem water: A model study. In review.
46. Swain, E.D.; Wolfert, M.A.; Bales, J.D.; Goodwin, C.R. Two-dimensional hydrodynamic simulation of surface-water flow and transport to Florida bay through the Southern Inland and Coastal Systems (SICS); U.S. Geological Survey Water-Resources Investigations Report 03-4287, U.S. Geological Survey: Reston, VA, USA, 2003.
47. Munns, R. Comparative physiology of salt and water stress. *Plant Cell Environ.* **2002**, *25*, 239–250.
48. Moreira, M.; Sternberg, L.D.L.; Martinelli, L.; Victoria, R.; Barbosa, E.; Bonates, L.; Nepstad, D. Contribution of transpiration to forest ambient vapour based on isotopic measurements. *Glob. Change Biol.* **1997**, *3*, 439–450.
49. Harwood, K.; Gillon, J.; Roberts, A.; Griffiths, H. Determinants of isotopic coupling of CO2 and water vapour within a Quercus petraea forest canopy. *Oecologia* **1999**, *119*, 109–119.
50. Passioura, J.B.; Ball, M.C.; Knight, J.H. Mangroves may salinize the soil and in so doing limit their transpiration rate. *Funct. Ecol.* **1992**, *6*, 476–481.
51. Hollins, S.E.; Ridd, P.V.; Read, W.W. Measurement of the diffusion coefficient for salt in salt flat and mangrove soils. *Wetl. Ecol. Manag.* **2000**, *8*, 257–262.
52. Herbert, D.A.; Rastetter, E.B.; Gough, L.; Shaver, G.R. Species diversity across nutrient gradients: an analysis of resource competition in model ecosystems. *Ecosystems* **2004**, *7*, 296–310.
53. Jiang, J.; DeAngelis, D.; Smith, T.J.I.; Teh, S.Y.; Koh, H.L. Spatial pattern formation of coastal vegetation in response to external gradients and positive feedbacks affecting soil porewater salinity: a model study. *Landsc. Ecol.* **2012**, *27*, 109–119.